Moroccan Journal of Chemistry
ISSN :2351-812X

Mor. J. Chem., 2023, Volume 11, Issue 03, Page 579-593
https://revues.imist.ma/index.php/morjchem
https://doi.org/10.48317/IMIST.PRSM/morjchem-v14i03.39198

Elucidating the inhibition behavior of *Pterocarpus santalinoides* leaves extract on mild steel corrosion in H_2SO_4 solution–GC-MS, FTIR, SEM, Experimental and computational approach

Eziuka J. E. [1], Onyeachu I. B. [1], Njoku D. I. [1], Nwanonenyi S. C. [1,2*], Chidiebere M. A. [1], Oguzie E. E. [1]

[1]*Africa Centre of Excellence in Future Energies and Electrochemical Systems (ACE-FUELS), Federal University of Technology Owerri, P.M.B. 1526, Nigeria*
[2]*Department of Polymer and Textile Engineering, Federal University of Technology Owerri, P.M.B. 1526, Nigeria*
**Corresponding author, Email address: simeonnwanonenyi@gmail.com*

Received *01 April 2023,*
Revised *30 April 2023,*
Accepted *02 May 2023*

Citation*: Eziuka J. E., Onyeachu I. B., Njoku D. I., Nwanonenyi S. C., Chidiebere M. A., Oguzie E. E. (2023)* Elucidating the inhibition behavior of *Pterocarpus santalinoides* leaves extract on mild steel corrosion in H_2SO_4 solution–GC-MS, FTIR, SEM, Experimental and computational approach*, Mor. J. Chem.,14(3), 579-593.*

Abstract: The drift towards the application of green inhibitors to mitigate acid corrosion of steel continues to encourage research into developing highly effective inhibitors derived from crude extracts of plant parts. The study investigates the inhibition behaviour of ethanol extract of Pterocarpus santalinoides (PS) against the corrosion of mild steel in 0.25 M H_2SO_4. Weight loss measurements showed that 1000 mg/l PS protected the steel with 88 % efficiency after 24 h immersion, which decreased to 47 % after 120 h immersion. Electrochemical impedance spectroscopy and potentiodynamic polarization measurements confirmed that PS extract is a mixed-type inhibitor and its adsorption lowers the double layer capacitance and rate of charge transfer at the steel-solution interface. The phenomenon blocks the steel surface damage based on SEM characterization. GC-MS and FTIR characterizations confirm that PS extract contain four major abundant phytoconstituents namely; benzeneacetaldehyde (BA), 2(5H)-furanone (FUR), ethyl 9,12,15-octadecatrienoate (EOD) and linoleic acid ethyl ester (LAEE). Molecular dynamic simulation (MDS) technique confirmed that individual molecules that formed the major parts of the extract contributed effectively in corrosion inhibition process in the order of EOD > LEAA > BA > FUR

Keywords: Corrosion inhibitor; Plant extract; *Pterocarpus santalinoides;* Mild steel; EIS

1. Introduction

Acid cleaning is an industrial process that is undertaken to rid metallic structural materials of inorganic scales which develop on their surfaces, over time, and interfere with their optimal performance. It is typically conducted using dilute mineral acids, especially, HCl and H_2SO_4. The inevitable corrosion attack simultaneously impacted on the underlying material by the acid is traditionally ameliorated by adding highly efficient corrosion inhibitors into the cleaning solution. Presently, there are stringent international regulations (Ahanotu *et al.,* 2022) which advocate for the use of greener and cheaper corrosion inhibitors as replacements for the highly-toxic and expensive alkylynic alcohol-based inhibitors currently used in many industries (Thakur *et al.,* 2013; Adama and Onyeachu *et al.,* 2022). Such green approach has been significantly achieved by adopting the use of crude extracts of plant biomass materials which are naturally abundant, readily available and exhibit near-zero toxicity (Verma *et al.,* 2018; Miralrio and Vázque, 2020; Alrefaee *et al.,* 2021)

The crude extracts of different plant parts have been reported as highly efficient inhibitors against the acid corrosion of different industrial metallic materials (Njoku *et al.,* 2016; Chidiebere *et al.,* 2016; Njoku *et al.,* 2021; Onuegbu *et al.,* 2020; Oguzie *et al*., 2012; Adindu *et al.,* 2016a; Maduabuchi, *et al.,* 2015; Singh, 2012; Okafor, Ebenso, and Ekpe, 2010; Adindu *et al.,* 2016b; Akalezi *et al.,* 2016; Awe *et al.,* 2015; Akalezi and Oguzie, 2016; Chidiebere *et al*, 2015). A review of the available literature reveals that the crude extracts are usually mixed-type inhibitors which have the capacity to block anodic and cathodic processes that sustain the corrosion. This is because the crude extracts are naturally endowed with different organic phytochemicals which possess the requisite moieties of a corrosion inhibitor (presence of electronegative hetero-elements like N, O, and S, and presence of C=C unsaturated bonds) that facilitate adsorption on the metal surface. Although much work has been done in the identification of different plant extracts as effective acid corrosion inhibitors, there is still serious lack of scientific information regarding the composition of their phytoconstituents and their individual characteristics and contribution to the overall inhibition impacted by the extract. This constitutes an obvious research gap in most reports of plant extracts as corrosion inhibitors.

Pterocarpus santalinoides (PS) is a legume plant that is native to tropical Western Africa. Its medicinal applications for the treatment of several skin diseases like eczema, candidiasis and acne are well documented (Osuagwu and Akomas, 2013). Reports of its pharmacological efficacy for the treatment of diabetes, cough and sore belly are also in the literature (Igoli *et al.,* 2005; Okwuosa *et al.,* 2011). From the perspective of corrosion, Ahanotu *et al.* (2020) compared the performance of water, ethanol, and methanol crude extracts of PS leaves, using detailed electrochemical and surface probe techniques. The authors confirmed that the corrosion inhibition followed the order: ethanolic extract > methanolic extract > aqueous extract. However, this work provides no evidence of the identity of individual molecules in PS leave extract and their plausible contributions to the overall corrosion inhibition by the extract.

Equipped with this observation, and the fact that ethanol extract of PS performs better than water and methanol extracts during acid corrosion of steel, we are motivated to undertake the present research. For this purpose, we investigate the inhibition performance of the ethanol extract of PS against the corrosion of mild steel after 24, 48, 72 96 and 120 h of immersion periods in 0.25 M H_2SO_4 solution by complementing detailed weight loss measurements with electrochemical (electrochemical impedance spectroscopy and potentiodynamic polarization) and surface probe (scanning electron microscopy) characterizations. Thereafter, we identify and characterize the phytochemical constituents of PS using gas chromatography-mass spectroscopy (GC-MS) and Fourier transform infrared (FTIR) spectroscopy. Finally, we apply computational modeling (molecular dynamics simulation and density functional theory) to screen the electronic properties and individual corrosion inhibition properties of the most abundant phytochemical constituents in the extract.

2. Methodology

2.1 Preparation and characterization of PS extract

The leaves of *Pterocarpus santalinoides* were obtained locally and identified at the Department of Crop Science Technology, School of Agriculture and Agricultural Technology, Federal University of Technology, Owerri. The leaves were washed, air-dried to constant weight and grinded into fine powder using an electric blender. Known mass of the powder was soaked in a round bottom flask containing 300 ml of ethanol, thoroughly mixed by shaking and allowed to stand for 72 h. The resulting mixture was filtered and the solvent content of filtrate was recovered with a rotary evaporator, so that

the solid mass obtained (whose mass was extrapolated from the known mass of leaves powder used) was used to prepare an inhibitor stock solution.

FTIR analysis of the extract was carried out over 400–4000 nm wavelength using Agilent Technology Cary 630 FTIR. The GC-MS characterization was analyzed using a gas chromatograph (Agilent 6890N) hyphenated with a mass spectrophotometer (5973B MSD) with Restek capillary column (30m x 0.25mm; film thickness 1.4 µm). The temperature was programmed as follows: Initial temperature was 40 ºC which increased to 150 ºC at the rate of 10 ºC/min. The temperature was again increased to 230 ºC at the rate of 5 ºC/min. The process continued till the temperature reached 280 ºC at the rate of 20 °C/min which was held for 8 minutes. The injector port temperature remained constant at 280 °C and detector temperature was 250 °C then. Helium was used as the carrier gas with a flow rate of 1 ml/min. Split ratio and ionization voltage were 110:1 and 70 eV respectively. To identify the unknown phytochemical components, present in the samples, their individual mass spectral peak value was compared with the database of National Institute of Science and Technology 2014. Then identification was done by comparing the unknown peak value and chromatogram from GC-MS against the known chromatogram peak value from the NIST Library database. Subsequently, the details about their molecular formula, molecular weight, retention time and percentage content were also obtained.

2.2 Corrosion inhibition assessment

Experiments were carried out on mild steel (MS) specimen with composition of 0.179 % C, 0.165 % Si, 0.439 % Mn, 0.203 % Cu, 0.034 % S and Fe (to balance). The steel bars were machined into weight loss coupons with dimensions 3 cm× 3cm × 1 cm. To prepare the sample, the coupons were abraded with emery papers of variable grades (400, 600, 800 and 1200 grades). The coupons were washed thoroughly with distilled water, degreased in absolute ethanol and dried in acetone and warm air. Weight loss measurements were conducted after 24, 48, 72, 96 and 120 h immersion of duplicate coupons in 200 ml solution of 0.25 M H_2SO_4 without and with 100, 250, 500 and 1000 mg/l PS concentrations. After each immersion time, the coupons were retrieved, cleaned according to ASTM G109 standard procedure (ASTM-G 01–03, 1997) and reweighed in order to determine weight loss (ΔW) based on Eq. (1). The electrochemical measurements, after 24 h immersion, provided mechanistic insight into the PS performance. Firstly, an open circuit potential (OCP) was established by allowing the coupons to freely corrode in the inhibited and uninhibited acid solution for 1 h. Electrochemical impedance spectroscopy (EIS) was performed by applying a sinusoidal signal amplitude of ± 10 mV over a frequency range of 10^5 Hz to 10^{-1} Hz. Potentiodynamic polarization (PDP) measurement was conducted by applying a potential perturbation of ± 250 mV vs. the OCP using a scan rate of 0.166 mV/s. Finally, scanning electron microscopy (SEM) was employed to peruse the surface morphology of the steel after the polarization in the acid solution without and with 1000 mg/l PS. A microscope JEOL JSM-6610 LV model operated at a voltage of 20 kV and irradiation current of 10 mA, was used for this purpose:

$$\Delta W = W_i - W_f \quad (1)$$

Where W_i = initial weight (g), W_f = final weight (g)

The percentage inhibition efficiency IE (%) was calculated using Eq. (2) as shown below:

$$IE = \left[1 - \frac{W_f}{W_1}\right] \text{ x } 100 \quad (2)$$

2.3 Computational modeling

The computational modeling approach adopted for the study was molecular dynamic simulation (MDS) based on the frame work of density functional theory (DFT) as contained in the Material studio software (BIOVIA, 2017). This was done to investigate the adsorption interactions between the molecules of the major chemical constituents of extract and metal surface. Thus, the electronic molecular structure of mild steel (Fe) imported into the 3D atomistic document from the structure document was geometrically optimized using the Forcite module tool. Then it was cleaved along (110) plane and enlarged to supercell of 10 x 8 simulation box to contain the required surface area for the interaction. In addition, the cleaved metal surface was built to crystal structure of 20.0 Å thickness and 1.00 Å position. The electrolytes (500 H_2O molecules, $5SO_4^{2-}$ ions and $5H_3O^+$ ions) were packed onto the surface of metal using adsorption locator module tool while the inhibitor molecule was docked onto the metal surface using docking tools. Furthermore, the geometrical optimization and quench dynamic simulation was performed on the prepared using Forcite module tool. The geometrically optimization was performed with the following parameters; COMPASS forcefield, electrostatic and van der Waals interactions via Ewald summation method, 1000 maximum iterations, algorithm (Smart), displacement (0.015Å), force (0.5 Kcal/mol/Å) and energy (0.001 kcal/mol). Quench dynamic simulation parameters include: quench steps (250), number steps (5000), 1fs time step, temperature (298 K), NVE ensemble and 5.0 ps total simulation time. Finally, the adsorption energy (or binding energy, E_{BE}) was obtained from the relationship expressed in the following Equation (3) (Nwanonenyi *et al.,* 2020; Njoku *et al.,* 2021; Rouifi *et al.,* 2019):

$$E_{BE} = E_{Total} - (E_{MSE} + E_{molecule}) \quad (3)$$

Where E_{BE}, E_{Total} and E_{MES} represents binding energy of interaction energy between the molecule and metal surface, total binding energy, binding energy of metal in the presence of electrolytes, and binding interaction energy of molecule respectively. The Equation (3) provides information on the forces of interaction existing at the interfacial level between metal crystal surface and inhibitor molecule in the presence of electrolytes.

3. Results and Discussion

3.1 Characterization of PS extract

The FTIR spectrum for the ethanol extracts of PS leaves is provided in Fig. 1. These major peaks strongly suggest that the PS extract is enriched with unsaturated oxygen-containing phytoconstituents which will, expectedly, interact with the metal surface using electrons delocalized around the C=C bonds and the electronegative oxygen (Wang *et al.,* 2019; Dehghani *et al.,* 2019; Dehghani, *et al.,* 2019a; Dehghani, *et al.,* 2019b; Dehghani *et al.,* 2019c). Up to 29 phytoconstituents were identified in the GC-MS result (see Table S1 in supplementary data). The four major peaks (based on peak intensity) correspond to benzeneacetaldehyde (BA), 2(5H)-furanone (FUR), Ethyl 9,12,15-octadecatrienoate (EOD), and linoleic acid ethyl ester (LAEE). These are highlighted in Table 1, and they confirm the FTIR observation of oxygen-rich constituents in the PS extract.

3.2 Experimental elucidation of PS as corrosion inhibitor

3.2.1 Weight loss result

Fig. 2(a) presents the plots of weight loss experienced by the steel during corrosion in 0.25 M H_2SO_4 without and with different concentrations of PS extract, between 24 and 120 h immersion at room temperature. Fig. 2(b) presents the corresponding inhibition efficiency delivered by the different PS concentrations after the different immersion times. (The table presenting the recorded values of

weight loss and the standard deviations is shown in the supporting document, as Table S2). The presented results clearly show that the steel corrosion was retarded by the addition of the plant extract. This retardation is rationally attributed to the adsorption of the different phytoconstituents in the plant extract. Their adsorption could be on anodic or cathodic (or both) reactive sites on the steel surface, depending on their chemical speciation in the acid solution. The adsorption blocks the oxidation of Fe → Fe^{2+}, which is the fundamental reaction that causes the weight loss of steel materials during corrosion (Elyoussfi *et al.,* 2019).

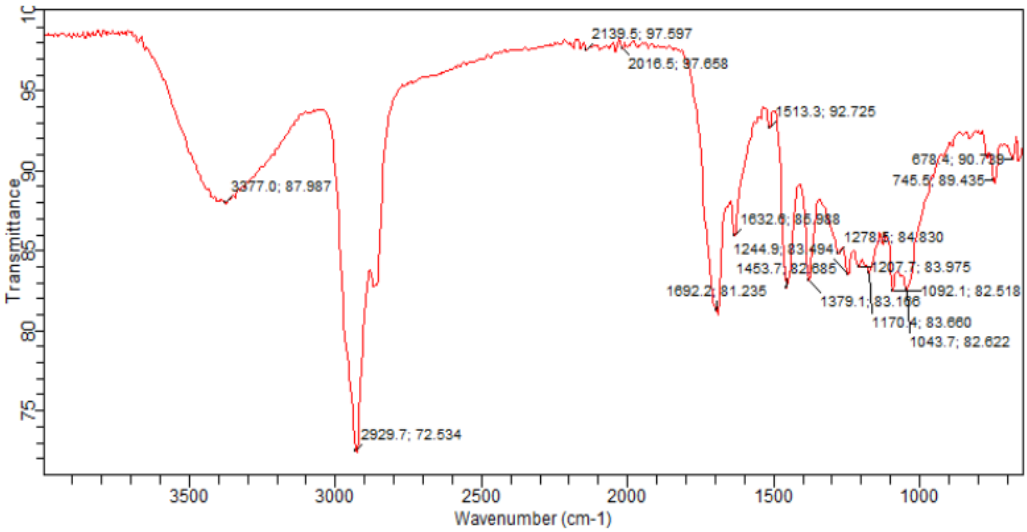

Fig. 1 FT-IR spectrum of *Pterocarpussantalinoides*leave extract

The surface protection impacted by PS is concentration-dependent. As can be seen, the addition of 1000 mg/l of PS decreased the weight loss from 0.7128 g to 0.0828 g after 24 h immersion, impacting the highest efficiency of 88.38 %. However, the performance of PS extract diminishes over prolonged immersion time. The results in Fig. 2 reveal that weight loss increases over the immersion times considered, while the inhibition efficiency decreases simultaneously. This observation, which is not different from previous reports (Ajayi, *et al.,* 2014; Mohammed *et al.,* 2021; Zakeri, *et al.,* 2022) can be attributed to the subtle degradation of the adsorbed inhibitor-substrate interface. During acid corrosion, steel cannot form protective passive layers. Rather, the most dominant product on steel surface, during acid corrosion, is reported to be Fe_3C (Crolet, *et al.,* 1998; Onyeachu *et al.,* 2019). It is a major component phase in steel and exhibits electronic characteristics whereby it acts as cathodic site that facilitates dissolution of Fe at anodic site. Its build up at the interface would definitely impair the integrity of inhibitor adsorption, causing some extent of desorption from the steel surface. This eventually allows penetration of the acid solution into the interface where the activity of H^+ is higher and Fe dissolution also increases.

The mode of adsorption of PS on the steel surface was investigated using different adsorption isotherms, among which the Langmuir isotherm gave the best fit. The Langmuir isotherm can be described according to Eq. (4); where C(mg/l) is the inhibitor concentration, K_{ads} is the adsorption equilibrium constant and θ(%IE/100) is the degree of surface coverage (Golchinvafa *et al.*, 2020). The Langmuir plot is provided in Fig. 3, and shows a linear relationship (with very high correlation coefficient) between C/θ and C. Such linearity indicates inhibitor adsorption as a monolayer film devoid of inhibitor-inhibitor interaction (Langmuir, 1932).

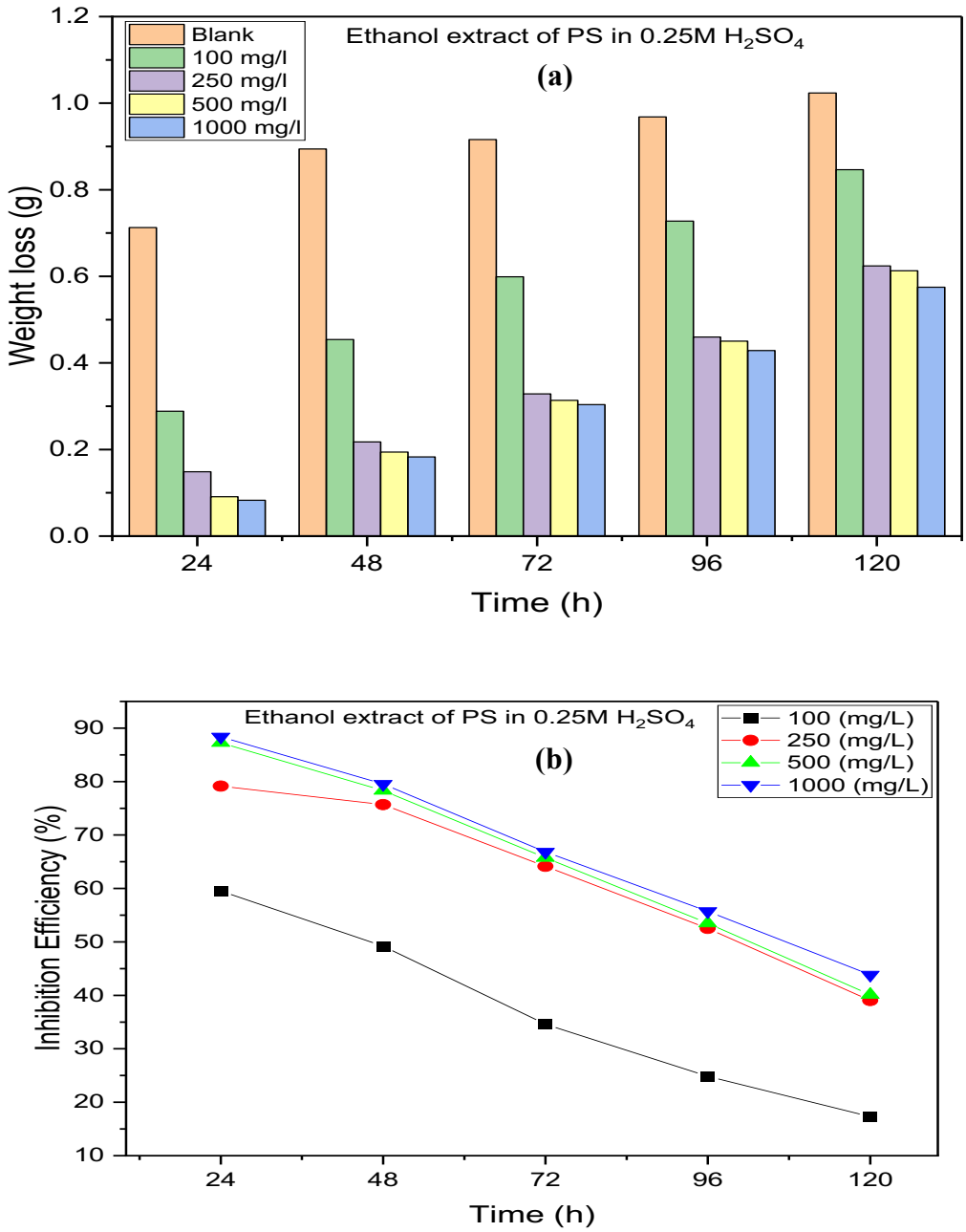

Fig. 2. Variation of (a) weight loss and (b) inhibition efficiency of ethanol extract of PS during steel corrosion in 0.25 M H_2SO_4 solution without and with different PS concentrations after 24 to 120 h immersion

The implication is that the phytoconstituents of PS extract occupy different sites available for the adsorption on the steel surface. So, they do not jostle for adsorption; a mechanism that could lead to formation of inhibitor layers. The value of K_{ads}, which is the reciprocal of the intercept of Langmuir plot, was used to calculate the value of free energy of adsorption according to Eq. (5); where R is the universal gas constant and T is the absolute experimental temperature. The negative value of ΔG_{ads} supports that the adsorption of inhibitor phytoconstituents is thermodynamically feasible and spontaneous:

$$\left[\frac{1}{K_{ads}}\right] + C = \frac{C}{\theta} \quad (4)$$

$$K_{ads} = \frac{1}{55.5} e^{\frac{\Delta G_{ads}}{RT}} \quad (5)$$

The determination of the free enthalpy in the case of natural plant extracts is the subject of several authors. In fact, the natural extract contains infinite compounds at different concentrations (Obot *et al.,* 2011; Bouknana *et al.,* 2014; Abdulbasit *et al.,* 2023). In this way, inhibitory action occurs is probably due to the synergistic intermolecular effect of the various constituents of the aqueous extract studied (Bammou *et al.,* 2010; Loukili *et al.,* 2022; Alimohammadi *et al.,* 2023).

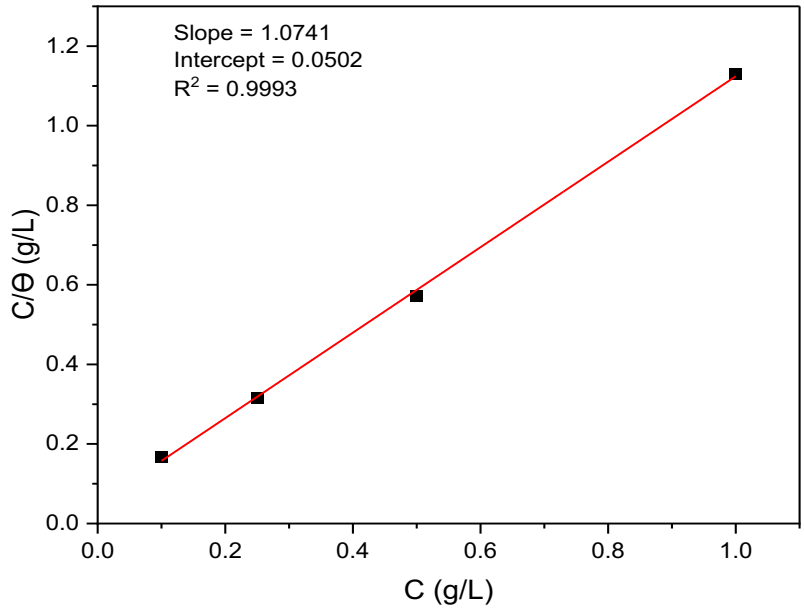

Fig.3 Langmuir adsorption isotherm for the adsorption of PS on the surface of the mild steel at room temperature

3.2.2 Electrochemical result

The traditional Nyquist and Bode absolute impedance plots have been presented in Fig. 4(a) and (b) to elucidate the EIS results acquired. The Nyquist arcs and low frequency values of absolute impedance are greater in the presence of PS extract, and are more enhanced with increase in PS concentration. This is an attestation to an improved resistance of the steel. The single time constant observed for all Nyquist shapes implies a purely activation-controlled corrosion mechanism which is controlled by dielectric characteristics of the steel-acid solution interface and the rate of charge transported within this interface. For this purpose, the corrosion mechanism is modelled using the simple Randle electric circuit in the inset of Fig. 4(b). The R_s and R_{ct}, respectively, represent the resistance of the solution and resistance to charge transfer within the interface. The constant phase element (CPE_{dl}) describes the dielectric characteristics of the interface. The *CPE* is composed of the admittance element (Y_o) and a roughness parameter α ($-1 \leq \alpha \leq 1$) (Hsu and Mansfeld, 2001; Onyeachu *et al.,* 2023). Its application in describing corrosion phenomena makes it possible to account for the fluctuating current response to the EIS perturbation, which arises from surface heterogeneity of the corroding surface. However, Y_o is inadequate to describe the double layer properties of the interface, compared with a double layer capacitance (C_{dl}). Both elements (Y_o and C_{dl}) are related according to the Eq. (6) [43]. Lower C_{dl} values and higher R_{ct} values are indicators of increased corrosion resistance. The values of all electrical elements are provided in Table 2:

$$C_{dl} = Y_o^{\frac{1}{\alpha}} \left[\frac{1}{R_s} + \frac{1}{R_{ct}}\right]^{\frac{\alpha-1}{\alpha}} \quad (6)$$

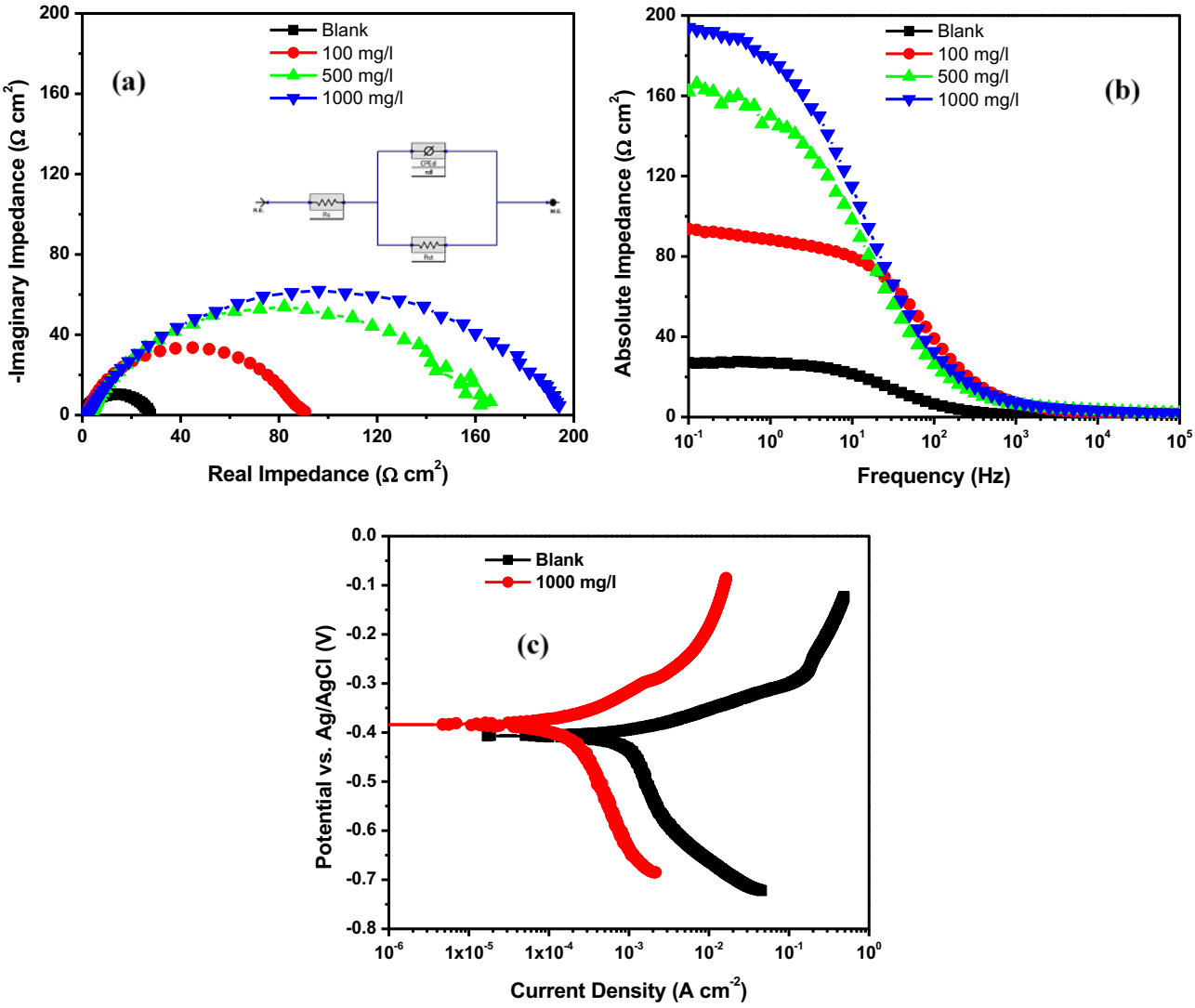

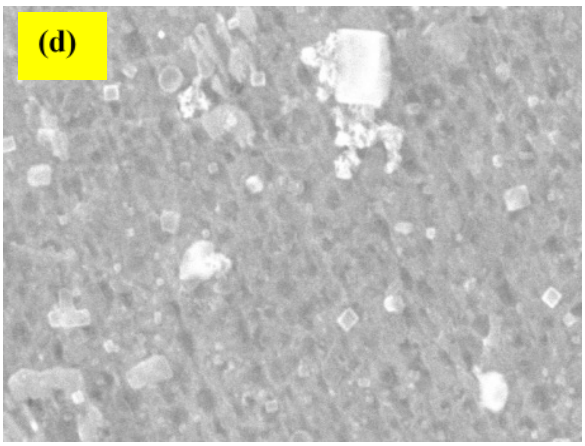

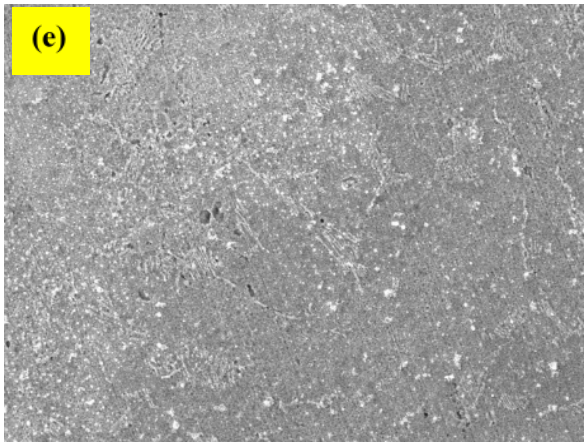

Fig. 4 Electrochemical measurement of mild steel corrosion after 24 h immersion in blank and PS-containing 0.25 M H_2SO_4 solution expressed in form of (a) nyquist (b) absolute impedance (c) potentiodynamic polarization and SEM surface morphologies for (d) uninhibited and (e) inhibited steel.

The dielectric and charge transfer properties are influenced by the types and quantity of charges occupying the interface. In the blank acid solution, the interface is enriched only with aqueous H^+ and SO_4^{2-} ions, both of which cause higher value of C_{dl} and the most severe corrosion attack evident in the least R_{ct} recorded in Table 2. In the inhibited acid solution, however, the PS phytoconstituents are

present within the interface. They do not trigger a different corrosion pathway, but improve the preferred corrosion pathway adopted by the steel. This is why the Nyquist shapes (and absolute impedance shapes) are similar both in the absence and presence of PS extract. The phytoconstituents present in the interface displace molecules of water and other aqueous corrosion-causing components like H^+ and $SO_{4(aq)}^{2-}$ (Brug *et al*., 1984). Hence, they diminish the C_{dl} and increase the R_{ct} consistently with increasing PS concentration. Considering that these phytoconstituents possess some similarity in their molecular structure (especially the presence of C=O and C=C bonds), it is rational to reason that the extent of displacement of aqueous components would be influenced by the charge and molecular size of the phytoconstituents. While the smaller sizes of BA and FUR could enable them permeate the interface towards the steel surface more freely with minimal steric hindrance, the larger sizes of EOD and LAEE could be favourable with respect to covering larger surface area once adsorbed. Nevertheless, the combined adsorption of these phytoconstituents increases the hydrophobicity of the steel surface and explains the decrease in C_{dl} and increase in R_{ct}, as Table 2 shows. It is remarkable to notice that the R_s also increases with PS concentration. Such increase, which is in agreement with previous observation (Yildiz *et al.,* 2018; Onyeachu *et al.,* 2022) has been attributed to increasing isolation of the corroding surface from the solution, as a result of the inhibitor adsorption. Additionally, the EIS trend agrees perfectly with the observation from weight loss whereby a sharp rise in efficiency occurs as PS concentration changes from 100 mg/l (69.64 %) to 500 mg/l (83.26 %), after which it does not significantly change at 1000 mg/l (86.64 %).

Potentiodynamic polarization curves obtained after 24 h immersion of the mild steel in the H_2SO_4 solution without and with 1000 mg/l PS extract are provided in Fig. 4(c). The technique elucidates the mechanism by which the phytoconstituents of PS extract influence the anodic and cathodic half-reactions at the steel-solution interface. In H_2SO_4 solution, $Fe \rightarrow Fe^{2+}$ will be the most dominant anodic reaction exhibited by steel, while $H^+ \rightarrow H_2$ is the most dominant cathodic reaction (Bouklah *et al.,* 2004). The presence of PS has no obvious effect on the corrosion potential (E_{corr}), and the shapes of the plots are also similar. This confirms the EIS observation that adsorption of PS extract only modifies the corrosion mechanism, but does not alter the preferred mechanism. However, PS shifts the anodic and cathodic current densities to lower values, which confirms that it lowers the rate of charge transfer at the steel-solution interface. The ability to lower both anodic and cathodic reactions makes PS extract a mixed-type corrosion inhibitor. The cathodic reactions are minimized courtesy of the competitive adsorption between the protonated PS constituents and H^+. Regarding this, a smaller-size molecule (like BA and FUR) could compete more favorably with H^+, than the larger EOD and LAEE. On the other hand, the protonated species can also lower anodic reaction by blocking the $Fe \rightarrow Fe^{2+}$ transition. They achieve this by donating reactive electrons (localized as lone pairs around oxygen, and as pi-electrons in C=C bonds) into the d-orbitals of Fe in order to create coordinate covalent bonds with inhibitor molecules. Otherwise, the anodic adsorption could occur via electrostatic attraction with anionic SO_4^{2-}already pre-adsorbed on the steel surface containing abundant Fe^{2+} ions. Regarding this, the presence of more C=C bonds in their linear chains (in addition to the C=O and C–O bonds) could enable EOD and LAEE to impact more anodic influence than BA and FUR. Nevertheless, the simultaneous adsorption of all phytoconstituents definitely ensures the mixed-type inhibition delivered by PS extract. The changes in anodic and cathodic Tafel constants, in Table 3, also confirm the dual-impact effect of the extract. This eventually lowers corrosion current density (i_{corr}) from 376.10 µA/cm^2 (in the blank) to 60.00 in the presence of 1000 mg/l PS, so that an inhibition efficiency of 83.90 % was achieved in agreement with EIS and weight loss results.

The surface of the polarized steel in the inhibited and uninhibited acid solution was perused to provide insight into the extent of microstructural protection offered by the PS extract on the corroding steel. In the blank solution, the SEM image in Fig. 4(d) reveal a seriously damaged and rough steel surface exhibiting general and pitting corrosion. The pits had small diameters with regular shapes, similar with the observations of Al-Moubaraki, Ganash and Al-Malwi, (2020). The inhibition protection offered by PS extract is further confirmed by the smoother surface profile of the steel in Fig. 4(e). The pits are not visible in the presence of PS and the surface damage is clearly mitigated

Table 2: EIS parameters obtained after 24 h corrosion of mild steel in 0.25 M H_2SO_4 solution without and with different PS concentrations

Conc. (mg/l)	R_s (Ω cm^2)	CPE_{dl} Y_o (μF cm^{-2}s^{n-1})	n	R_{ct} (Ω cm^2)	C_{dl} (μF cm^{-2})	IE (%)
Blank	1.32	560	0.87	26.90	189.32	–
100	1.37	92	0.84	88.60	17.51	69.64
500	1.83	145	0.84	160.70	36.17	83.26
1000	2.08	54	0.85	201.35	10.83	86.64

Table 3: Polarization parameters obtained after 24 h corrosion of mild steel in 0.25 M H_2SO_4 solution without and with 1000 mg/l PS.

Conc. (ppm)	E_{corr} (mV/Ag/AgCl)	i_{corr} (μA/cm^2)	β_a (mV/Decade)	β_c (mV/Decade)	IE (%)
Blank	–407	376.10	64.70	170.00	–
1000	–384	60.00	57.30	132.60	83.90

3.2.3 Computational modeling result

GC-MS result revealed that major chemical constituents of *Pterocarpussantalinoides* leaf extract include the following; benzeneacetaldehyde, 2(5H)-Furanone, Ethyl 9,12,15-octadecatrienoate and Linoleic acid ethyl ester. Thus, the adsorption of these molecules and metal (Fe) crystal surface was determined using theoretical approach (molecular dynamic simulation) to proffer better understanding of the forces of interaction between them. This interaction was simulated under gaseous and solvated phases respectively in order to approximate the real-life experimental conditions and evaluate the response of corrosive agents on the adsorption characteristics of the molecules involved. Fig. 5 presents the side views of the most stable adsorption configurations between the metal surface and different molecules involved in a simulated gaseous and solvated environment. Clearly, each molecule adsorbed in a horizontal orientation on the metal surface and this signifies favourable interaction. It is believed that the different functional groups present within the structure of each molecule either donated lone pair of electrons which partially filled empty d-orbital or π-electron cloud which contributed in the formation co-ordinated bond or interaction that provided the stable interfacial film for metal protection. In fact, the stable film changes the surface chemistry of the metal structure by closing or blocking prevalent active corrosion sites on the surface of metal. In addition, it is possible that protonated molecule and some non-polar regions in the inhibitor molecule could combine to feature hydrophobic characteristics which can displace adsorbed water molecules from the surface of metal and ensure effective protection of the metal (Nwanonenyi *et al.*, 2020). Adsorption or binding energy parameter evaluates the forces of interfacial interaction existing between metal surface and inhibitor molecule. The increase in the negative value of binding energy of interaction suggests stronger metal-inhibitor

interaction and more spontaneous process (Farhadian *et al.,* 2021). The results of binding energy obtained for interaction between BA, FUR, EOD and LAEE molecule respectively and metal crystal surface in both gaseous and solvated phase respectively is presented in Table 4. The order inhibition effectiveness based on the result of binding energy of interaction is as follow; EOD > LEAA > BA > FUR

Adsorption interaction	Gaseous Phase	Solvated Phase
Metal surface + BA Molecule	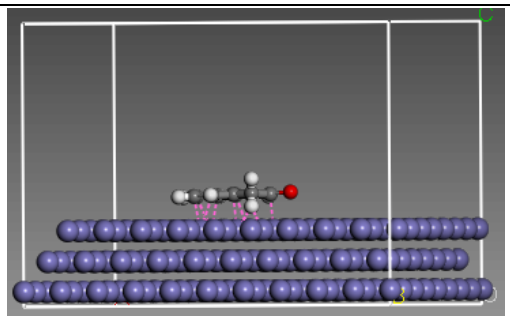	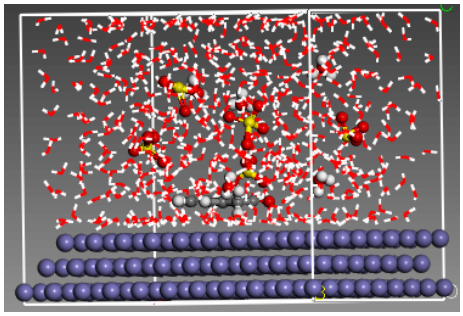
Metal surface + FUR Molecule	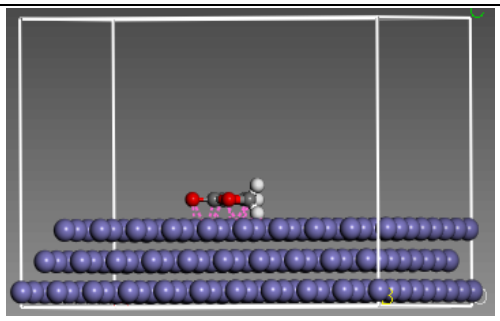	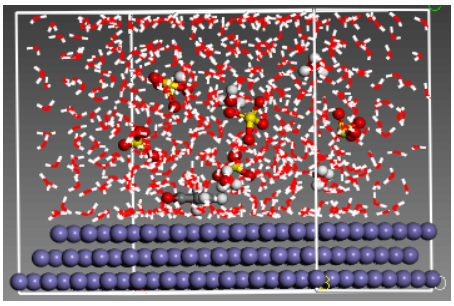
Metal surface + EOD Molecule	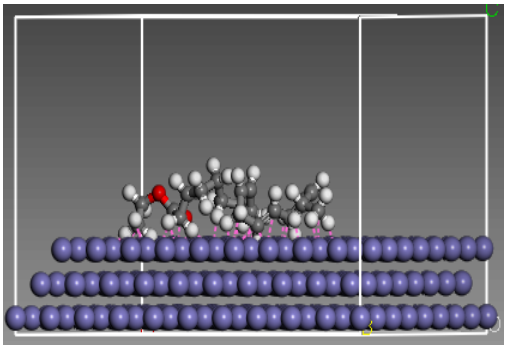	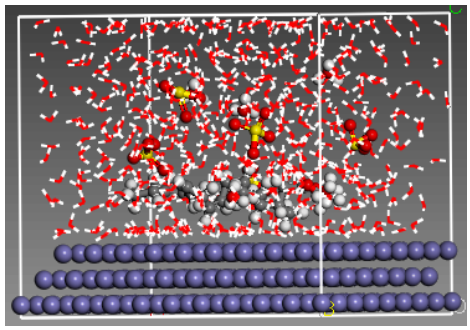
Metal surface + LAEE Molecule	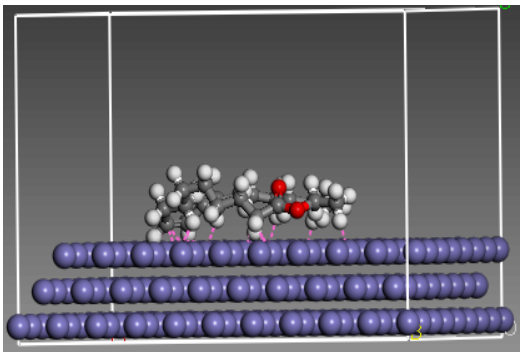	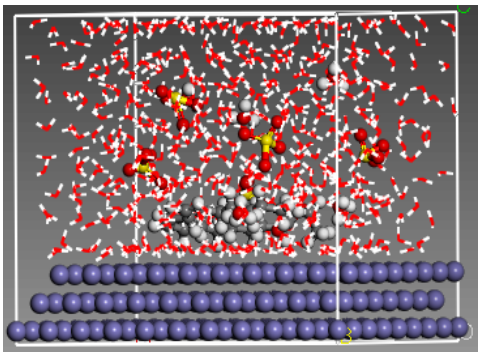

Fig. 5 Different side views of the most stable adsorption configurations of BA, FUR, EOD, and LAEE molecule and mild steel in both gaseous and solvated phase respectively.

Table 4: Result of binding energy of interaction between BA, FUR, EOD and LEAA molecule and metal (Fe) crystal surface in gaseous and solvated phase respectively

Adsorption interaction	Gaseous phase kcal/mol	Solvated phase kcal/mol
Metal surface + BA Molecule	-109.9814	-27.6742
Metal surface + FUR Molecule	-80.1819	-13.0409
Metal surface + EOD Molecule	-237.2756	-95.4753
Metal surface + LEAA Molecule	-225.0126	-64.3210

Conclusion

Developing green and highly efficient corrosion inhibitors based on crude extracts of plant biomass is imperative for industrial sustenance. Not only this, proper identification of the plant phytochemicals responsible for the corrosion inhibition and the plausible individual inhibition characteristics of these phytochemicals are also important. In the work, the ethanol extract of *Pterocarpus santalinoides* (PS) was investigated as inhibitor against the corrosion of mild steel in 0.25 M H_2SO_4. Detailed weight loss measurements, over different times up to 120 h, were complemented with electrochemical measurements, surface characterization and computational modeling. The following conclusions can be drawn from the results obtained:

1. Ethanol extract of PS is a highly efficient corrosion inhibitor for mild steel corrosion in H_2SO_4 solution but its efficiency decreases with time
2. Its phytochemicals adsorb on both anodic and cathodic sites on the steel surface, thus, impacting a mixed-type inhibition characteristics on the extract
3. Its major phytochemicals are benzeneacetaldehyde (BA), 2(5H)-Furanone (FUR), Ethyl 9,12,15-octadecatrienoate (EOD) and Linoleic acid ethyl ester (LAEE);
4. Theoretically, the corrosion inhibition contribution determined by phytochemicals is in the order: EOD > LEAA > BA > FUR.
5. FTIR, GC-MS and SEM characterization confirmed the results of experimental findings.

Acknowledgement: The authors wish to acknowledge the financial support from the World Bank Africa Centers of Excellence for Impact (ACE Impact), Project No. NUC/ES/507/1/304

Disclosure statement: *Conflict of Interest:* The authors declare that there are no conflicts of interest.
Compliance with Ethical Standards: This article does not contain any studies involving human or animal subjects.

References

Abdulbasit Y.U., Abdullahi B. U. and Bishir U. (2023) Experimental and theoretical evaluation of corrosion inhibition performance of *Senna obtusifolia* leaves extract on mild steel in 0.5M HCl, *Mor. J. Chem.,* 14(2), 282-299. Doi: https://doi.org/10.48317/IMIST.PRSM/morjchem-v11i2.38203

Adama K.K and Onyeachu I.B., (2022) The corrosion characteristics of SS316L stainless steel in a typical acid cleaning solution and its inhibition by 1-benzylimidazole: Weight loss, electrochemical and SEM characterizations, *Journal of the Nigerian Society of Physical Sciences,* 4, 214–222.

Adindu B., Ogukwe C., Eze F and Oguzie E.E. (2016a) Exploiting the Anticorrosion Effects of Vernonia Amygdalina Extract for Protection of Mild Steel in Acidic Environments, *J. Electrochem. Sci. Technol.,* 7(4), 251-262.

Adindu C.B., Oguzie E.E. and Ogukwe C.E. (2016b) Corrosion inhibition of mild steel in 0.5 M H_2SO_4 using ethanol extract of Funtumia elastic, *International Letters of Chemistry, Physics and Astronomy,* 68, 24-38.

Ahanotu C.C., Onyeachu I.B., Solomon M.M., Chikwe I.S., Chikwe O.B and Eziukwu C.A. (2020) Pterocarpussantalinoides leaves extract as a sustainable and potent inhibitor for low carbon steel in a simulated pickling medium, *Sustainable Chemistry and Pharmacy,* 15, 100196

Ahanotu C. C., Madu K. C., Chikwe I. S and Chikwe O. B. (2022) The inhibition behaviour of extracts from Plumeria rubra on the corrosion of low carbon steel in sulphuric acid solution, *J. Mater. Environ. Sci.,* 13(9), 1025-1036

Ajayi O.M., Odusote J.K and Yahya R.A. (2014) Inhibition of mild steel corrosion us Jatropha Curcas leaf extract, *J. Electrochem. Sci. Eng.* 4(2), 67-74

Akalezi C.O., Ogukwe C.E., Ejele E.A and Oguzie E.E. (2016) Mild steel protection in acidic media using Mucunapruriens seed extract, *Int. J. Corros. Scale Inhib.,* 5(2) (2016) 132–146.

Akalezi C.O and Oguzie E.E. (2016) Evaluation of anticorrosion properties of *Chrysophyllum albidum* leaves extract for mild steel protection in acidic media, *Int. J. Ind. Chem*., 7, 81–92.

Alimohammadi M., Ghaderi M., Ramazani S.A., A. et al. (2023). Falcaria vulgaris leaves extract as an eco-friendly corrosion inhibitor for mild steel in hydrochloric acid media. *Sci. Rep.* 13, 3737 https://doi.org/10.1038/s41598-023-30571-6

Al-Moubaraki A.H., Ganash A.A. and Al-Malwi S.D (2020) Investigation of the Corrosion Behavior of Mild Steel/H_2SO_4 Systems, *Mor. J. Chem.* 8(1), 264-279. https://doi.org/10.48317/IMIST.PRSM/morjchem-v8i1.19249

Alrefaee S.H., Rhee K.Y., Verma C., Quraishi M.A., Ebenso E.E. (2021) Challenges an advantage of using plant extract as inhibitors in modern corrosion inhibition systems: Recent advancements, *Journal of Molecular Liquids*, 321, 114666.

ASTM-G 01–03, (1997) Standard practice for preparing, cleaning, and evaluation corrosion test specimens, ASTM Book of Standards

Awe F.E., Idris S.O., Abdulwahab M and Oguzie E.E. (2015) Theoretical and experimental inhibitive properties of mild steel in HCl by ethanolic extract of *Bosciasene galensis*, *Cogent Chemistry,* 1, 1112676

Bammou, L. et al. (2010) Thermodynamic properties of Thymus satureioides essential oils as corrosion inhibitor of tinplate in 0.5 M HCL: Chemical characterization and electrochemical study. *Green Chem. Lett. Rev.* 3, 173–178

Bouklah M., Hammouti B., Aouniti A., Benhadda T. (2004) Thiophene derivatives as effective inhibitors for the corrosion of steel in 0.5 M H2SO4, *Progress in organic coatings* 49(3), 225-228

Bouknana D., Hammouti B., Messali M., Aouniti A., Sbaa M. (2014), Phenolic and non-Phenolic Fractions of the Olive Oil Mill Wastewaters as Corrosion Inhibitor for Steel in HCl medium, *Port. Electrochim. Acta,* 32, 1-19

Brug G.J., van den Eeden A.L.G., Rehbach M.S and Sluyters J.H. (1984) The analysis of electrode impedances complicated by the presence of a constant phase element, *J. Electroanal. Chem. Interfacial Electrochem,* 176, 275–295.

Chidiebere M.A., Oguzie E.E., Liu L., Li Y and Wang F. (2015) Inhibitory Action of Funtumia elastica Extracts on the Corrosion of Q235 Mild Steel in Hydrochloric Acid Medium: Experimental and Theoretical Studies, *Journal of Dispersion Science and Technology*, 36, 1115–1125.

Chidiebere M., Nnanna L., Adindu B.C., Oguzie K., Benlonwu O., Onyeachu I.B and Oguzie E.E. (2016) Inhibition of Acid Corrosion of Mild Steel Using Delonixregia Leaves Extract, *International Letters of Chemistry, Physics and Astronomy,* 69, 74–86

Crolet J. Thevenot N and Nesic S. (1998) Role of conductive corrosion products in the protectiveness of corrosion layers, *Corrosion* 54 (1998) 194–203

Dehghani A., Bahlakeh G., Ramezanzadeh B and Ramezanzadeh M. (2019) Potential of Borage flower aqueous extract as an environmentally sustainable corrosion inhibitor for acid corrosion of mild steel: electrochemical and theoretical studies. *J. Mol. Liq.* 277, 895–911.

Dehghani A. Bahlakeh G. and Ramezanzadeh B. (2019) Green Eucalyptus leaf extract: a potent source of bio-active corrosion inhibitors for mild steel. *Bioelectrochemistry*, 130, 107339.

Dehghani A. Bahlakeh G and Ramezanzadeh B. (2019) A detailed electrochemical/ theoretical exploration of the aqueous Chinese gooseberry fruit shell extract as a green and cheap corrosion inhibitor for mild steel in acidic solution. *J. Mol. Liq.* 282, 366–384.

Dehghani A., Bahlakeh G., Ramezanzadeh B and Ramezanzadeh M. (2019) A combined experimental and theoretical study of green corrosion inhibition of mild steel in HCl solution by aqueous Citrullus lanatus fruit (CLF) extract. *J. Mol. Liq.* 279, 603–624.

Elyoussfi A., Dafali A., Elmsellem H., Steli H., bouzian Y., Cherrak K., El Ouadi Y., Zarrouk A., Hammouti B. (2016), Adsorption and corrosion inhibition of new synthesized quinoline on mild steel in HCl and H_2SO_4 solutions, *J. Mater. Environ. Sci.* 7(9), 3344-3352

Farhadian A., S.A. Kashani S.A., Rahimi A., Oguzie E.E., Javidparvar A.A., Nwanonenyi, S.C., Yousefzadeh S and Nabid M.R. (2021) Modified hydroxyethyl cellulose as a highly efficient eco-friendly inhibitor for suppression of mild steel corrosion in a 15% HCl solution at elevated temperatures, *Journal of Molecular Liquids,* 338, 116607

Golchinvafa A., Anijdan S.H.M., Sabzi M and Sadeghi M. (2020) The effect of natural inhibitor concentration of Fumaria officinalis and temperature on corrosion protection mechanism in API X80 pipeline steel in 1 M H_2SO_4 solution. *International Journal of Pressure Vessels and Piping,* 188, 1-27.

Hsu C.H and Mansfeld F. (2001) Technical note: concerning the conversion of the constant phase element parameter Y_o into a capacitance, *Corros.* 57, 747

Igoli J.O., Ogaji O.G., Tor A.A and Igoli N.P. (2005) Traditional medicinal practice amongst the Igede people of Nigeria, Part II, Afr. J. Tradit. *Complementary Altern. Med.* 2(2), 134–152.

Langmuir I. (1932) Vapor pressures, evaporation, condensation and adsorption. *J. Am. Chem. Soc.* 54, 2798–2832

Loukili E. H., Azzaoui K., Author J. O., Author V., Hammouti B. (2022) Corrosion Inhibition using Green Inhibitors: An Overview, *Maghr. J. Pure & Appl. Sci.,* 8(2), 82-93. DOI: https://doi.org/10.48383/IMIST.PRSM/mjpas-v8i1.29392

Maduabuchi C.A., Oguzie E.E., Liu L., Li Y and Wang F. (2015) Adsorption and corrosion inhibiting effect of riboflavin on Q235 mild steel corrosion in acidic environments, *Materials Chemistry and Physics* 156, 95-104.

Miralrio A and Vázquez E.A. (2020) Plant extracts as green corrosion inhibitors for different metal surfaces and corrosive media: a review, *Processes,* 8(8), 942.

Mohammed N.J., Othman N.K., Taib M.F.M., Samat M.H and Yahya S. (2021) Experimental and Theoretical Studies on Extract of Date Palm Seed as a Green Anti-Corrosion Agent in Hydrochloric Acid Solution, *Molecules*, 26(12), 3535.

Njoku D.I., Ukaga I., Onyeachu I.B., Oguzie, E.E., Oguzie K.L and Ibisi N. (2016) Natural products for materials protection: Corrosion protection of aluminum in hydrochloric acid by Kola nitida extract, *Journal of Molecular Liquids*, 219, 417–424.

Njoku D.I., Njoku C.N., Lgaz H., Okafor P.C., Oguzie E.E and Li Y. (2021) Corrosion protection of Q235 steel in acidic-chloride media using seed extracts of Piper guineense, *Journal of Molecular Liquids,* 330, 115619.

Nwanonenyi S.C., Ezeani E.O., Obele C.M., Arinze C.V., Chidiebere M.A and Oguzie E.E. (2020) Protection of carbon steel surface in extreme environment using polymer mixture: effects of time, inhibitor concentration, mixing ratio and synergy, *Safety in Extreme Environments*, https://doi.org/10.1007/s42797-021-00029-x

Nwanonenyi S.C., Obasi H.C., Udochukwu U., Chidiebere M.A., Njoku D.I and Oguzie E.E. (2021) Protection by a polymer composite on carbon steel surface in 1.0 M HCl environment: a combined experimental and theoretical approach, *Brazilian Journal of Chemical Engineering*, https://doi.org/10.1007/s43153-021-00187-2

Obot I.B., Umoren S. A., Obi-Egbedi N.O. (2011) Corrosion inhibition and adsorption behaviour for aluminuim by extract of Aningeria robusta in HCl solution: Synergistic effect of iodide ions, *J. Mater. Environ.*

Sci. 2 (1), 60-71

Oguzie E. E., Adindu C. B., Enenebeaku C. K., Ogukwe C. E., Maduabuchi C. A and Oguzie K. L. (2012), Natural Products for Materials Protection: Mechanism of Corrosion Inhibition of Mild Steel by Acid Extracts of Piper guineense, *J. Phys. Chem. C,* 116, 13603−13615.

Okafor P.C., Ebenso E.E and Ekpe U.J. (2010) Azadirachta indica extracts as corrosion inhibitor for mild steel in acid medium, *Int. J. Electrochem. Sci.,* 5(7), 978-993.

Okwuosa C.N., Unekwe P.C., Achukwu P.U., Udeani T.K.C and Ogidi U.H. (2011) Glucose and triglyceride lowering activity of Pterocarpus santaniloides leaf extracts against dexamethasone induced hyperlipidemia and insulin resistance in rats, *Afr. J. Biotechnol.* 10(46), 9415–9420.

Onuegbu I.V., Oguzie E.E and Amadi S.A (2020) Electrochemical, SEM, GC-MS and FTIR study of inhibitory property of cold extract of *Theobroma cacao* pods for mild steel corrosion in hydrochloric acid, *International Journal of Engineering Trends and Technology (IJETT),* 68, (2020) 82-87.

Onyeachu I.B., Obot I.B., Sorour A.A and Abdul-Rashid M.I. (2019) Green corrosion inhibitor for oilfield application I: Electrochemical assessment of 2-(2-pyridyl) benzimidazole for API X60 Steel under sweet environment in NACE brine ID196, *Corrosion Science,* 150, 183–193.

Onyeachu I.B., Solomon M.M., Adama K.K., Nnadozie F., Ahanotu C.C., Akanazu C.E and Njoku D.I (2022) Exploration of the potentials of imidazole-based inhibitor package for heat exchanger- type stainless steel during acid cleaning operation, *Arabian Journal of Chemistry* 15 (2022) 103837.

Onyeachu IB., Njoku D.I., Nwanonenyi S.C., Ahanotu C.C and Etiowo K.M. (2023) Investigation into the adsorption and inhibition properties of sodium octanoate against CO_2 corrosion of C1018 carbon steel under static and hydrodynamic conditions, *Scientific African* 20, e01603.

Osuagwu G.G.E. and Akomas C.B. (2013) Antimicrobial activity of the leaves of three species of Nigerian Pterocarpus (Jacq.), *Int. J. Med. Aromatic Plants*, 3(2), 178–183.

Rouifi Z., Benhiba F., Faydy M. El., Laabaissi T., About H., Oudda H., Warad I., Guenbour A., Lakhrissi B and Zarrouk A. (2019). Performance and computational studies of new soluble triazole as corrosion inhibitor for carbon steel in HCl, *Chemical Data Collections*, 22, 100242. https://doi.org/10.1016/j.cdc.2019.100242

Singh M. R. (2012) A green Approach: A corrosion inhibition of mild steel by adhatodavasica plant extract in 0.5 M H_2SO_4, *Environments,* 10, 19.

Thakur S.A., Flake G.P., Travlos G.S., Dill J.A., Grumbein S.L., Harbo S.J and Hooth M.J. (2013) Evaluation of propargyl alcohol toxicity and carcinogenicity in F344/N rats and B6C3F1/N mice following whole-body inhalation exposure, Toxicology, 314(1), 100-111

Verma C., Ebenso E.E., Bahadur I and Quraishi M.A. (2018) An overview on plant extracts as environmental sustainable and green corrosion inhibitors for metals and alloys in aggressive corrosive media, *Journal of molecular liquids,* 266, 577-590.

Wang Q., Tan B., Bao H., Xie Y., Mou Y., Li P., Chen D., Shi S., Li X and Yang W. (2019) Evaluation of Ficustikoua leaves extract as an eco-friendly corrosion inhibitor for carbon steel in HCl media. *Bioelectrochemistry* 128 (2019) 49–55.

Yildiz M., Gerengi H., Solomon M.M., Kaya E and Umoren S.A. (2018) Influence of 1-butyl-1-methylpiperidinium tetrafluoroborate on St37 steel dissolution behavior in HCl environment. *Chem. Eng. Commun,* 205, 538–548.

Zakeri A., Bahmani E and Aghdam A.S.R. (2022) Plant extracts as sustainable and green corrosion inhibitors for protection of ferrous metals in corrosive media: A mini review, *Corros. Commun,* 5, 25-38.